Motion Control, Robotics,
Sensors, Simulation,
User application experiences

Pavol SPANIK[1]
Peter FIBICH[1]
Marek PASKALA[1]
Viktor BOBEK[1]
Peter SINLER[1]

USAGE OF MEMS SENSORS FOR THE SPEED CONTROL OF THE INDUSTRIAL TRANSPORT VEHICLE

It is possible to increase the productivity using the machines with their own intelligence. The drive characteristic of the autonomous industrial vehicle could be optimized by the modern MEMS sensors. During the drive are recorded and processed data from the build-in sensors through microprocessor. The drive characteristic is improved to obtain the optimal speed, safety and reliability according the recorded data.

ZASTOSOWANIE CZUJNIKÓW MEMS DO KONTROLI PRĘDKOŚCI W PRZEMYSŁOWYCH POJAZDACH TRANSPORTOWYCH

Istnieje możliwość wzrostu produktów przy użyciu maszyn o własnej inteligencji. Autonomiczna charakterystyka przemysłowych pojazdów może być optymalizowana poprzez nowoczesne czujniki MEMS. Podczas przejazdu są rejestrowane dane z wbudowanych czujników poprzez mikroprocesor.
Charakterystyka przewozu jest udoskonalana celem otrzymania optymalnej prędkości, bezpieczeństwa i niezawodności zgodnie z zarejestrowanymi danymi.

1. INTRODUCTION

The paper presents a short introduction to MEMS sensors, our implementation of the drive algorithm and an experimental measurement on simple testing track. In the modern factories actually are in use many machines with their own intelligence. That is one of the reasons why the productivity is growing. Other opportunities to increase the productivity are the usage of Electro-Mechanical Systems (MEMS) and the poweful microprocessors. With the assistance of MEMS sensors and microprocessors it is possible to shorten the goods transport between the place of production and the store. Actually is not so rarely usage of the autonomous transport vehicle. It transports the goods through the checkpoints along the selected track. Usually the speed of transport vehicle is constant. MEMS sensors could be use to map the track and adjust the speed of the vehicle to shorten the transportation time and to drive safely.

[1]University of Zilina, Faculty of Electrical Engineering, Department of Mechatronics and Electronics SLOVAKIA; Zilina 010 26, Univerzitna 8215/1.

2. MICRO-ELECTRO-MECHANICAL SYSTEMS (MEMS) [1]

MEMS stand for Micro-Electro-Mechanical Systems which integrates mechanical units and electronic components together through micro-fabrication technology at the sub-millimeter scale. With this technology, we can build microstructures through micro-machining and create sensors which are very small in size. There are several different methods for sensing motion.

2.1 Principle of the accelerometer

The MMA7361L is a low power, low profile capacitive micromachined accelerometer featuring signal conditioning, a 1-pole low pass filter, temperature compensation, self test, 0g-Detect which detects linear freefall, and g-Select which allows for the selection between 2 sensitivities. Zero-g offset and sensitivity are factory set and require no external devices.

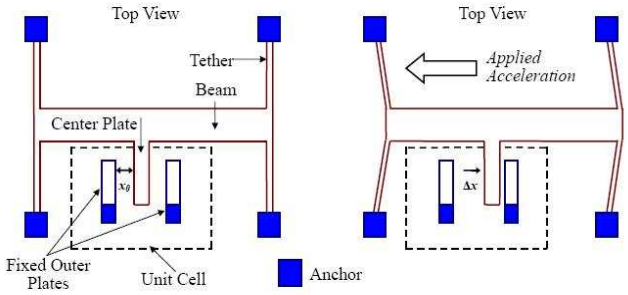

Fig.1. The Working Principle of a MEMS Accelerometer [1]

There are polysilicon springs inside the sensor which are used to suspend a beam over the surface of a silicon wafer and provide a resistance against applied force as shown in

Fig.1. When acceleration is applied to the sensor, according to the Hooke's law, the beam deflects as described in Equation (1) and a differential capacitor is used to measure the distance of the beam deflected as shown in Equation (2). Finally, we can further measure the applied acceleration which is proportional to the deflection of the beam as described in Equation (3)

$$\Delta d = \frac{F}{k} \tag{1}$$

$$\Delta C \approx C_0 \frac{\Delta d}{d_0} \tag{2}$$

$$a = \frac{F}{m} = \frac{k\Delta d}{m} \tag{3}$$

where: F is the applied force
k is the spring constant of tether
Δd is deflection of the beam
a is the applied acceleration,
m is mass of the beam

C_0 is the capacitance of the unit cell measured at stationary
C is the change in capacitance during force is applied
d_0 is the separation between the planes at stationary.

2.2 Principle of a MEMS Gyroscope

The gyroscope is an instrument which is used to measure angular velocity of a target mounted object. There is a bimorph vibrator inside the instrument as shown in Fig.2(b)

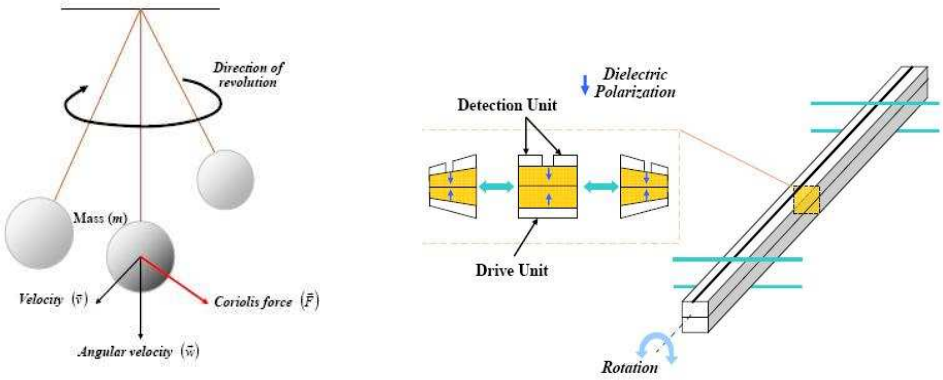

(a) Foucault's Pendulum *(b) Structure of Gyroscope*

Fig.2. The Working Principle of a MEMS Gyroscope [1]

which resonates with linear velocity $v_{vibration}\cos(\Omega t)$. If the sensor is fixed to the target body rotating at rate ω_{input}, the vibrator inside experiences a timevarying Coriolis acceleration as shown in Equation (4) and Fig.2(a). The acceleration is at the same frequency as the driving acceleration, but at right angles to the vibrator velocity. Hence, the magnitude of the applied rotation about the axis orthogonal to vibrator can be determined by measuring the Coriolis acceleration generated.

$$a_{coriolis}(t) = \lfloor -2\omega_{input} \otimes v_{vibration} \rfloor \tag{4}$$

where: $a_{coriolis}(t)$ is the Coriolis acceleration at time instant t
ω_{input} is the input angular velocity
$v_{vibration}$ is the linear velocity of the vibrator.

2.3 Application of the motion sensors

For the position computation is possible to use also an accelerometer or an encoder. With accelerometer can be measured actual acceleration in all three axes. Recalculation to the inertial system is necessary due to accelerometer is related/connected by the chassis. Negative influence of the vibration is eliminated by the either software or hardware filtering. Using encoder to obtain the position is easiest compared to accelerometer position

computation. Count of the impulses is proportional to the position. Gyroscope sense the angular velocity. Double integration is used to determine the yaw angle. Yaw angle is needed to translate into the inertial system [5].

3. IMPLEMENTATION OF OUR ALGORITHM

We had two ideas how to map the track. The first idea was to create map of the centrifugal forces. We can calculate velocity and position from centrifugal forces. The acceleration is the rate of the time change of the velocity of an object. At the same time, the velocity is the rate of change of the position of that same object. In other words, the velocity is the derivative of the position and the acceleration is the derivative of the velocity [3], thus:

$$a = \frac{dv}{dt} and\_v = \frac{ds}{dt} \therefore a = \frac{d(ds)}{dt^2} \tag{5}$$

where: a(t) – acceleration
v(t) – velocity
s(t) – position

The integration is the inverse of the derivative. If there is known of the acceleration of an object we can obtain the positional data by two successive integration of acceleration (assumed initial conditions zero):

$$v = \int (a)dt\_and\_s = \int (v)dt \therefore \int \left(\int (a)dt \right) dt \tag{6}$$

Inertial system permits to carry out the actual position relative to start point of the track. We can calculate actual position, velocity and direction from measured acceleration and angular velocity.

$$\varphi(t) = \int \omega(t)dt \tag{7},$$

where: φ(t) – angular position
ω(t) – angular velocity

From actual angular position and actual position difference in all three axes we can calculate position difference in the inertial system [4].

$$\begin{pmatrix} \Delta x \\ \Delta y \\ \Delta z \end{pmatrix} = \begin{pmatrix} \cos(\gamma).\cos(\alpha) & -\sin(\gamma).\cos(\beta) & -\cos(\alpha).\sin(\beta).\sin(\gamma) \\ -\sin(\gamma).\sin(\alpha).\sin(\beta) & & +\sin(\alpha).\cos(\gamma) \\ \sin(\beta).\sin(\alpha).\cos(\gamma) & \cos(\gamma).\cos(\beta) & \cos(\gamma).\sin(\beta).\cos(\alpha) \\ -\cos(\alpha).\sin(\gamma) & & +\sin(\gamma).\sin(\alpha) \\ \cos(\beta).\sin(\alpha) & -\sin(\beta) & \cos(\beta).\sin(\alpha) \end{pmatrix} \begin{pmatrix} \Delta x''' \\ \Delta y''' \\ \Delta z''' \end{pmatrix} \tag{8}$$

where: α – pitch $\Delta x'''$ - actual position in x-axis Δx - actual position in inertial x-axis

γ – yaw	$\Delta y'''$ - actual position in y-axis	Δy - actual position in inertial y-axis
β – roll	$\Delta z'''$ - actual position in z-axis	Δz - actual position in inertial z-axis

4. EXPERIMENTAL MEASUREMENT

A simple testing track was used to prove the computation of the position. The ellipse shape of the track was built. The accelerometer has measured the accelerations in two axes. The angular velocity ω was measured by the gyroscope. Measured data was filtered out by simple first-order lowpass filter. During the ride all the data was saved into the serial EEPROM. After one lap the data was read from EEPROM to the PC via BDM. Embedded board and PC were interfaced via freemaster software environment. All calculations were done in Matlab.

The measured angular velocity ω is depicted in the next Fig.3. The yaw angle θg was computed by Equation (9).

$$\theta_g(t) = \int \omega(t) dt \tag{9}$$

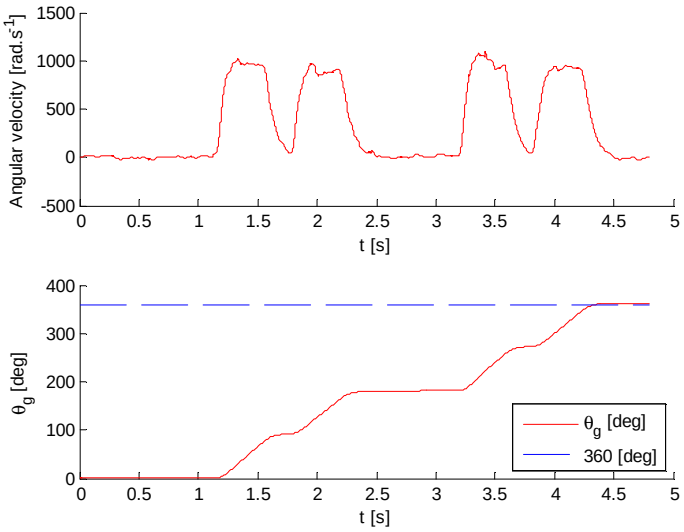

Fig.3. Angular velocity ω(t) and angle θg(t)

The variable realAcc is calculated from the measured voltage equivalent to the acceleration.

$$realAcc = \frac{acc \cdot ADC_{ref} \cdot g}{ADC_{res} \cdot ACC_{sens}} = \frac{acc \cdot 3.3 \cdot 9.81}{4095 \cdot 0.8} = 9{,}942 \cdot 10^{-3} \cdot acc \tag{10}$$

where: acc – measured acceleration in the particular axis

ADC_{ref} – ADC voltage reference voltage

g – gravitational acceleration

ADC_{res} – resolution of the ADC

ACC_{sens} – accelerometer sensitivity pre Volt

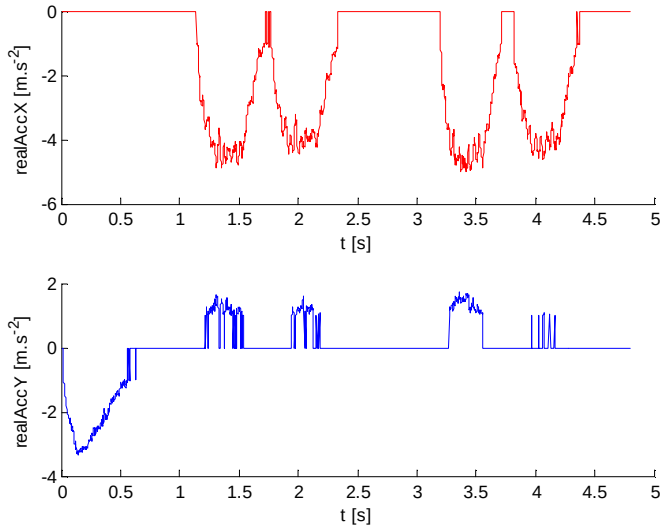

Fig.4. Computed real acceleration in X and Y axis

StacAccX/Y is the translated acceleration into the inertial system.

$$stacAccX = realAccX \cos\left(\frac{\pi \cdot \theta_g}{180}\right) + realAccY \sin\left(\frac{\pi \cdot \theta_g}{180}\right) \tag{11}$$

$$stacAccY = -realAccX \sin\left(\frac{\pi \cdot \theta_g}{180}\right) + realAccY \cos\left(\frac{\pi \cdot \theta_g}{180}\right) \tag{12}$$

The integrals was discreted using Forward Euler Method.

$$Speed = \int stacAccXdt \;\Rightarrow\; Speed[n] = Speed[n-1] + stacAccX.\Delta T \tag{13}$$

$$Position = \int Speeddt \Rightarrow\; Position[n] = Position[n-1] + Speed.\Delta T \tag{14}$$

Sensor error around the zero was eliminated by hysteresis as shown in the sample of the code.

```
for i=1:length(accX)
   if(and(accX(i)<100 ,accX(i)>-100))
      accX_0(i)=0;
   else
      accX_0(i)=accX(i);    end
   if(and(accY(i)<100 ,accY(i)>-100))
      accY_0(i)=0;
   else
      accY_0(i)=accY(i);    end
end
```

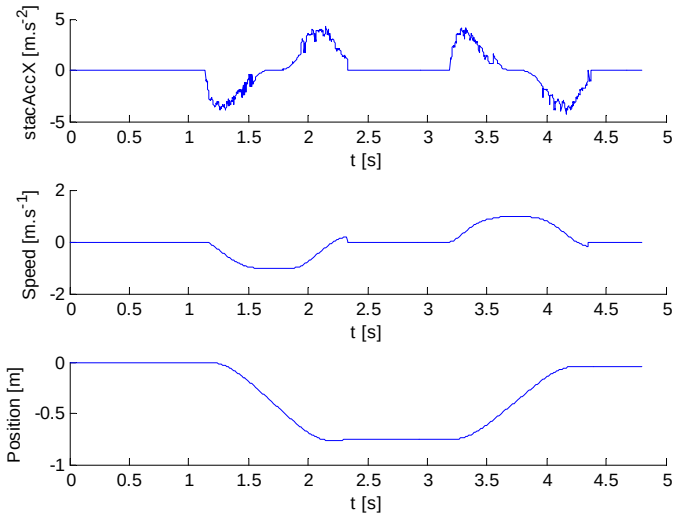

Fig. 5. Acceleration, speed and position in X axis related to the origin

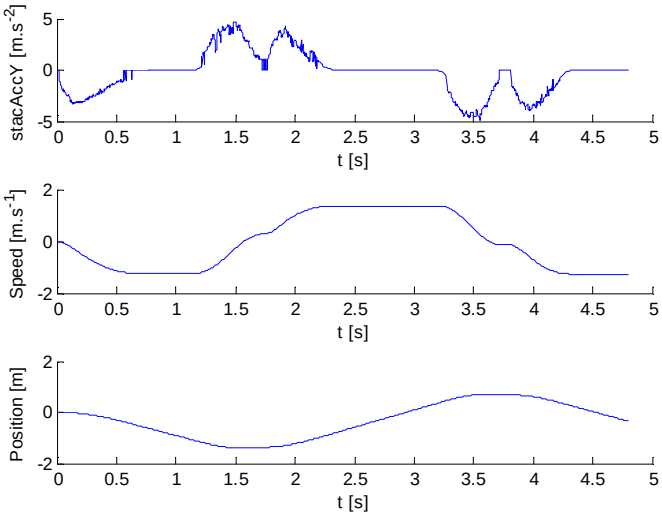

Fig. 6. Acceleration, speed and position in Y axis related to the origin

The computation inaccuracy/error has been caused with neglect of the sensor drift and tilt compensation in X, Y axes. The position error in X axis after one lap has been 5cm. Because of the simplifications ride on more complicated tracks was not so reliable with this method.

$$Speed = \int stacAccXdt \Rightarrow Speed[n] = Speed[n-1] + stacAccX.\Delta T \quad (13)$$

$$Position = \int Speeddt \Rightarrow Position[n] = Position[n-1] + Speed.\Delta T \quad (14)$$

Sensor error around the zero was eliminated by hysteresis as shown in the sample of the code.

```
for i=1:length(accX)
   if(and(accX(i)<100 ,accX(i)>-100))
      accX_0(i)=0;
   else
      accX_0(i)=accX(i);    end
   if(and(accY(i)<100 ,accY(i)>-100))
      accY_0(i)=0;
   else
      accY_0(i)=accY(i);    end
end
```

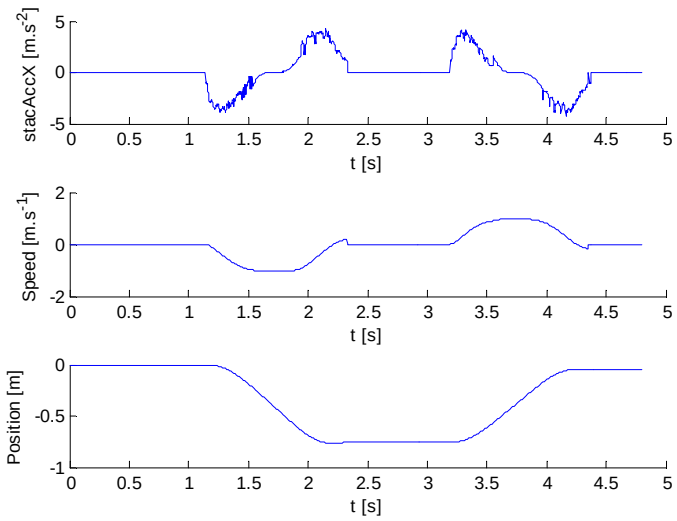

Fig.7. Acceleration, speed and position in X axis related to the origin

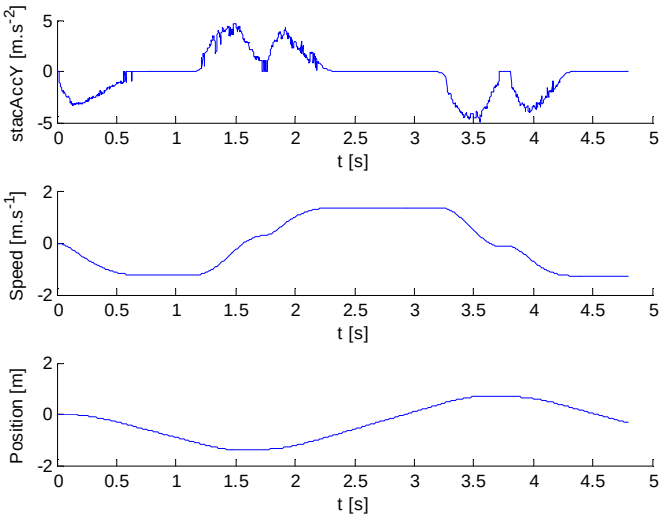

Fig.8. Acceleration, speed and position in Y axis related to the origin

The computation inaccuracy/error has been caused with neglect of the sensor drift and tilt compensation in X, Y axes. The position error in X axis after one lap has been 5cm. Because of the simplifications ride on more complicated tracks was not so reliable with this method.

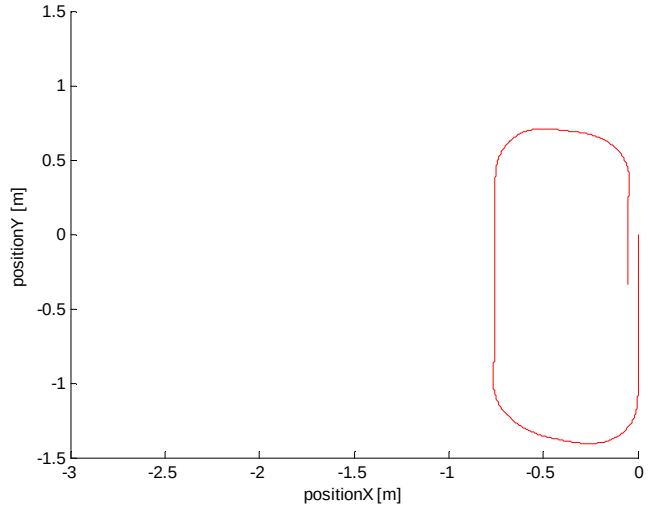

Fig.9. Computed shape of the track

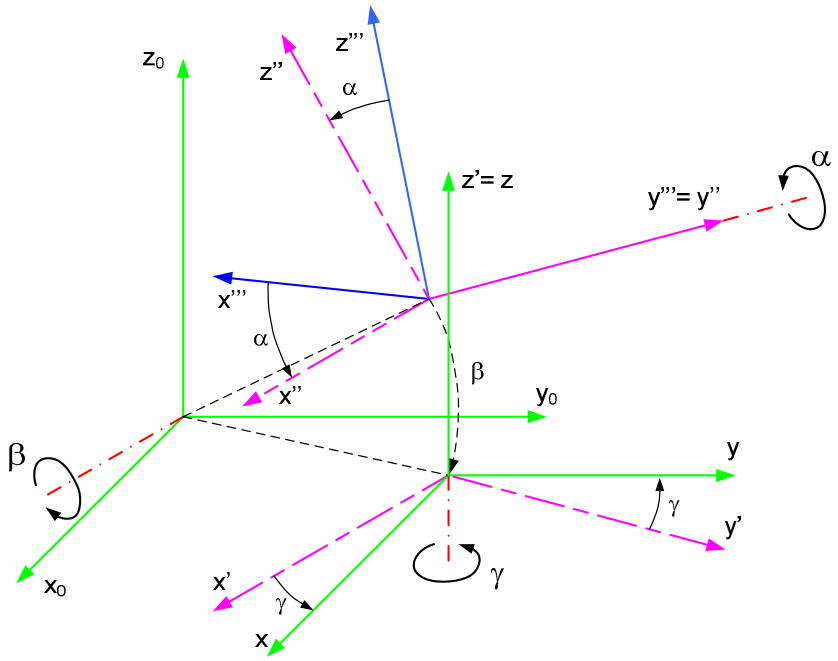

Fig.10. Within the inertial system point movement

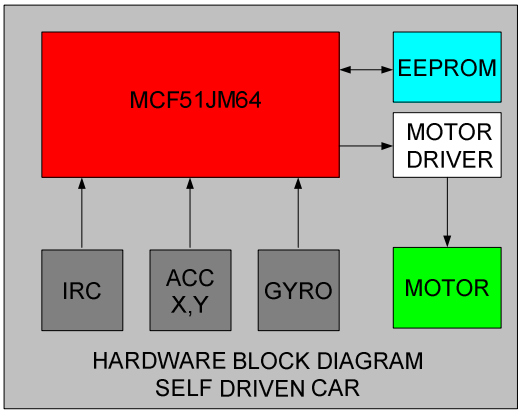

Fig.11. Hardware block diagram of the self driven car

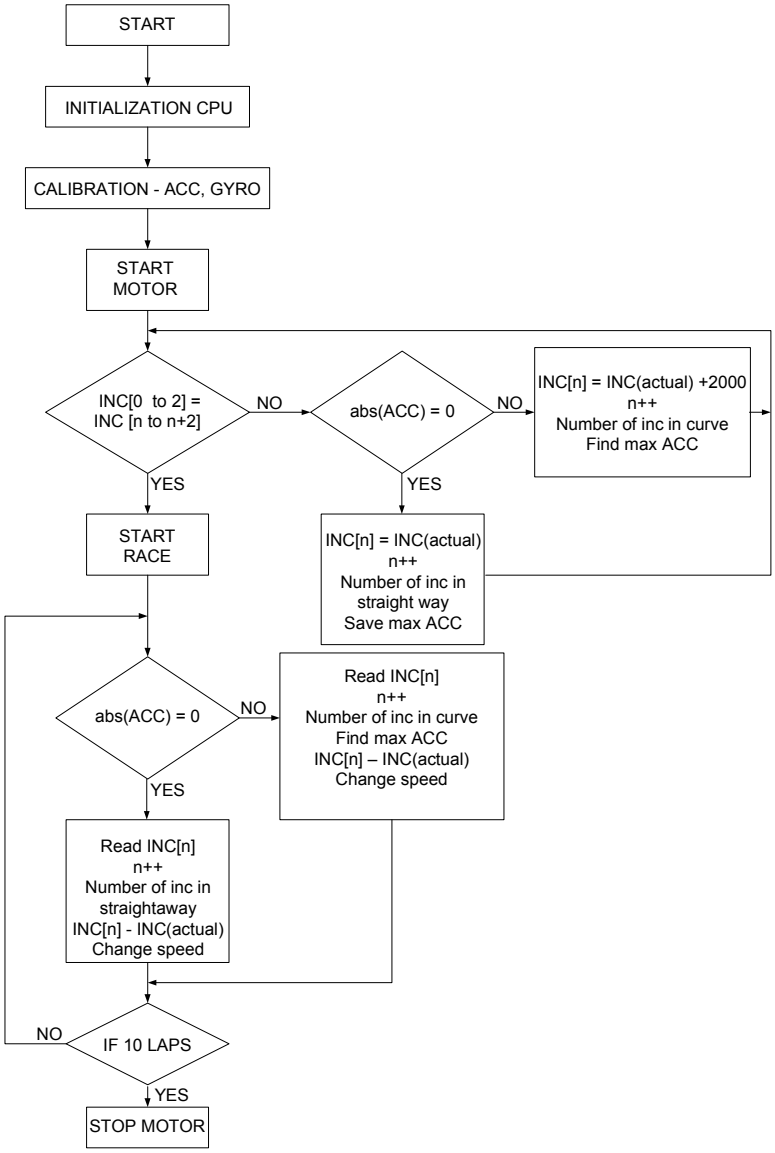

Fig.12. Block diagram of the algorithm

Second idea was to measure centrifugal force at the curves and lengths of straight ways. From centrifugal force we can calculate maximal speed of the slot car. From the lengths of the straight ways we can calculate how soon we should brake. Fig.12. shows block diagram of the algorithm. Fig.11. shows the hardware of the self driven car. After first three saved segments we compare them with last three segments. We have added constant to all curves

to recognize them from straight ways. The positive constant 2000 was used for right curves and negative one for the left ones. When it was found three same segments as at the beginning of the track, then we are in second lap. We use saved data for safe and fast drive. The microcontroller reads from the memory saved data in advance to brake safely.

5. CONCLUSION

This paper presents two methods how to map the unknown track. First method is more complicated due to two successive integration of the filtered acceleration, but it's more suitable for the 3D track. Second method demands less computation power, but it constrains another opportunities to improve the algorithm. During the race was used second method, due to more reliable results. For the next Freescale Race Challenges we will use first methods because of the 3D track. Potentially we can combine both methods.

6. REFERENCES

[1] Tsang, C. C.: Error Reduction Techniques for a MEMS Accelerometer-based Digital Input Device, March 2008, The Chinese University of Hong Kong, pp. 6-7
[2] Freescale Semiconductors.: ±1.5g, ±6g Three Axis Low-g Micromachined Accelerometer
[3] Seifert, K., Camacho, O.: "Implementing Positioning Algorithms Using Accelerometers", Application Note AN3397
[4] Doskocil, E.: "Equipment for Inertial Navigation.", in czech, Bachelor thesis, CVUT, 2006, pp. 3-5
[5] Príkopová, A, Kállay, F: New approaches in logic circuit synthesis, ATP journal, Bratislava, ISSN 1335-2237, Roč.X, č.6(2003)

7. ACKNOWLEDGEMENT

The authors wish to thank for the financial support to VEGA Agency for the project No. 1/0470/09, and R&D operational program Centre of excellence of power electronics systems and materials for their components No. OPVaV-2008/2.1/01-SORO, ITMS 26220120003 funded by European regional development fund (ERDF) and Slovak Research and development Agency for the financial support of project "Development of a high-voltage module assigned for traction applications" No. APVV-20-051705